IEEE Access
Multidisciplinary ⋮ Rapid Review ⋮ Open Access Journal

Received March 13, 2021, accepted April 6, 2021, date of publication April 14, 2021, date of current version April 21, 2021.

Digital Object Identifier 10.1109/ACCESS.2021.3072420

Short-Term Prediction in Vessel Heave Motion Based on Improved LSTM Model

GANG TANG[1], JINMAN LEI[1], CHENTONG SHAO[1,2], XIONG HU[1], WEIDONG CAO[3], AND SHAOYANG MEN[4]

[1]Logistics Engineering College, Shanghai Maritime University, Shanghai 201306, China
[2]Aviation Key Laboratory of Science and Technology on Fault Diagnosis and Health Management, Shanghai 201601, China
[3]Research Center of Fluid Machinery Engineering and Technology, Jiangsu University, Zhenjiang 212013, China
[4]School of Medical Information Engineering, Guangzhou University of Chinese Medicine, Guangzhou 510006, China

Corresponding author: Shaoyang Men (shaoyang.men@gzucm.edu.cn)

This work was supported in part by the National Natural Science Foundation of China under Grant 82004259, in part by the GuangDong Basic and Applied Basic Research Foundation under Grant 2020A1515110503, and in part by the Young Talent Training Project of Guangzhou University of Chinese Medicine under Grant QNYC20190110.

ABSTRACT In order to solve the problem of control performance degradation caused by time delay in wave compensation control system, predicting vessel heave motion can be the input vector of the control system to alleviate time delay problem. The vessel heave motion belongs to the problem of time series, this paper proposes an improved Long Short-Term Memory (LSTM) model with a random deactivation layer (dropout), which can deal with the time series problem very well. In order to obtain the vessel heave motion, this paper establishes a wave model suitable for marine operation, and solves the vessel heave motion through the mathematical model of vessel motion. Finally, the paper predicts the vessel heave motion in a short predicted time series. In the process of obtaining the prediction effect of vessel heave motion, the Back Propagation (BP) neural network and the standard LSTM neural network are used to compare with the improved LSTM neural network. While the predicted time series is 0.1 s at sea state 3, the mean absolute percentage (MAPE) errors of BP neural network in the prediction of vessel heave motion is $1.06 \times 10^{-2}\%$, the standard LSTM in the prediction of heave motion is $1.43 \times 10^{-4}\%$, the improved LSTM in the prediction of heave motion is $7.51 \times 10^{-6}\%$. The improved LSTM improves MAPE by $1.05 \times 10^{-2}\%$ compared with the BP and $1.42 \times 10^{-4}\%$ compared with the standard LSTM. The prediction results show that the improved LSTM has a strong prediction capability with not easily overfitted in vessel heave motion prediction. The results show that the improved LSTM provides a new idea for vessel motion prediction and solves the problem of time delay, which is useful for the study of stability in marine operations.

INDEX TERMS Short-term prediction, improved long short-term memory (LSTM), vessel heave motion, time delay.

I. INTRODUCTION

Due to the existence of winds, waves, the safe and stable driving of vessels at sea are different from that of cars on land. The complex marine environment cause vessels multi-degree of freedom motion, includes heave motion, surge motion, sway motion, and so on. The vessel heave motion limits the accuracy of the equipments' installation and orientation on the sea surface, affecting the marine operation's safety and efficiency seriously [1]. Because of the above reasons, researches on vessel heave motion are necessary. To reduce the environmental conditions' influence on the marine operation, the series-parallel mechanism was proposed to compensate the motion of the cargo on the vessels [2]. However, the compensation accuracy of the vessels motion can be severely affected due to the apparent time delay of wave compensation devices [3], especially in the active control system. To solve the problem of time delay, some methods were presented to predict vessels motion. By taking the prediction results as the input of the control system, the compensation of cargo movement in advance can reduce the unnecessary fluctuation caused by environmental factors [4].

Recently, predictions of vessel heave motion have been studied widely. Methods for vessel motion prediction can be divided into three categories, including physics-based numerical methods [5], data-driven methods [6], and combination

The associate editor coordinating the review of this manuscript and approving it for publication was Haiyong Zheng.

methods of physics-based numerical and data-driven [7]. The numerical methods use mathematical models to describe the variation of vessel motion based on physical conditions and processes, which are sophisticated and difficult to solve. Because that of the mathematical models with many interference factors, some prediction effects are not ideal. As a result, fewer and fewer scholars use physics-based numerical methods recently. The data-driven methods learn patterns from historical observations and further use the learned patterns to predict future vessels motion. The common strategies are real-time prediction [8]–[10], and short-term prediction [11]. The machine learning-based prediction models were used for the real-time vessels motion prediction to their capability in nonlinearity processing. The real-time prediction has high accuracy and strong robustness. However, the real-time predictions have high requirements for the control system, and the control processes are more complex [12]. The real-time estimations of vessels motion have been researched in [13], [14]. Compared with the real-time prediction, the offline prediction can also achieve good prediction results. The short-term prediction is one of many offline predictions, it can satisfy the prediction accuracy and reduce the problem of low control accuracy caused by time delay in vessel motion prediction [15]. The combined methods of physics-based numerical and data-driven have the advantages of both. It can obtain better prediction results through the establishment of a simple mathematical model without large datum. Traditional methods have the physics-based numerical methods and some data-driven methods like classical time series models, which have poor prediction effects with complex model [16].

Some intelligent learning models like the neural network models can effectively improve the prediction accuracy with simple models, which also have advantages in vessel motion prediction. Since the 1990s, some scholars had used neural networks to identify the vessel coupled heave and pitch motion [17]. After, many neural network algorithms were applied in vessel motion prediction, including the Back Propagation (BP) neural network [18], Autoregressive Model (AR) model [6], Radial Basis Function (RBF) neural network [12], [19], [20], Support Vector Regression (SVR) neural network [4], [21], Wavelet Neural Network (WNN) [22], and so on. The above studies have shown that a given prediction model's predictability is affected by the characteristics of the vessel motion sequence.

Recurrent Neural Networks (RNNs) are effective ways to process time series. The vanishing and exploding gradient problems cannot build model of long-term dependencies in the vessel motion sequence well. For this shortage, in 1997, Hochreiter and Schmidhuber [23] proposed Long Short-Term Memory (LSTM), which was one of the time-recurrent neural networks. The LSTM can remember information for much longer periods of time due to its recurrent structure and gating mechanisms. It is regarded as a state-of-the-art method for time series related problems [24], [25]. The LSTM is a popular RNN in recent years [26]. As described in [27], the behaviors of LSTM were similar to dynamic systems. By using gate units, LSTM has avoided the problems of gradient degradation and learning long-term patterns. LSTM is the basic cell of multiple models [28], many scholars gradually optimize LSTM neural network [29]. However, in the field of wave compensation, over-optimization can lead to overfitting.

With the advantage of the networks remembering inputs for a long time and an explicit memory, LSTM has been widely applied in many areas, especially in time series modeling, like predictions of sea waves [30] and vessel motion [11]. In this paper, a short-term prediction study about the vessel heave motion based on an improved LSTM model with dropout has been proposed in marine operations. In the process of vessel motion prediction, it has become a development direction to study the response of the vessel to the wave [31].

Many theoretical methods of vessel motion modeling in waves have been proposed by many scholars, including approximate empirical formula [32], spectral interpolation, two-dimensional theory, three-dimensional theory, computational fluid dynamics considering the fluid viscosity, and so on. Strip theory is a common method to study the response of vessels to waves [33]. In the strip theory, the vessel is regarded as a slender body. Taking a small length of the cross-section to calculate the two-dimensional effect of fluid on the cross-section each time, ignoring the interference of hydrodynamic force along the vessels length direction. Integrating the calculated fluid effect on each cross-section along the vessels length, finally the forces of fluid on the whole vessel are obtained.

The remainder of this paper is organized as follows. The improved LSTM applied to predict impact vessel heave motion is described in Section II. The wave model is established by a two-parameter spectrum and vessel motion is established by strip theory in Section III. To study the influence of short-term prediction, the neural networks' prediction effects on vessel motion at different time delays are discussed in Section IV. By comparing with other algorithms, the effectiveness of the improved LSTM algorithm is illustrated. Finally, the conclusion is presented in Section V.

II. LSTM APPLIED TO PREDICT VESSEL HEAVE MOTION

This Section mainly includes the description of algorithm flow, the introduction of the improved LSTM model, and the setting of some parameters.

A. DESCRIPTION OF ALGORITHM FLOW

There are strong correlations and dependencies between vessel heave sequences. The current vessels heave motion are affected by the previous motion and affecting the next moment. In this respect, the time series methods can be used in predicting future motion. The time series methods can analyze and characterize the relations of the vessel heave motion between the sequence values. The time series methods which are predicting the future values based on the past sequence values of vessel heave motion is used in this paper. To solve the problem of connecting to remote data,

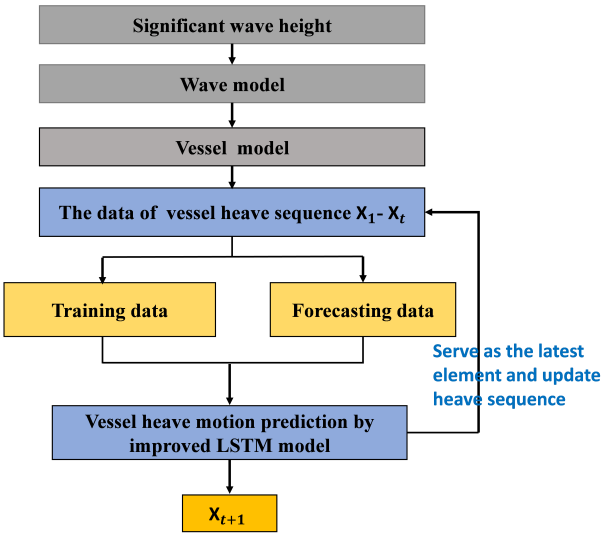

FIGURE 1. Algorithm flow in the vessels heave motion prediction.

the improved LSTM can extract the dependence between data from time-series data.

The algorithm flow in vessel heave motion prediction is shown in Fig.1. By setting different significant wave heights, the wave models under different sea conditions are established. By the establishment of vessels' motion model based on strip theory, the vessels motion sequence which is responded to different sea conditions is obtained. By taking the "Yuming" vessel as an example, through the mathematical model for solving vessel motion, the vessel heave motion sequence is obtained. Then the paper divides the obtained heave sequence datum into training datum and predicting datum. The training datum is used to train the improved LSTM model, predicting datum can be obtained by the trained model. The heave sequence in a time window form is first input into improved LSTM for independent predictions. Next, their predictions on each horizon are combined through averaging to produce the final prediction. The final prediction is used as the latest element of the input heave sequence to update the heave sequence, which is further used to predict one more time series. By repeating the above process, vessel heave motion predictions can be obtained.

B. THE IMPROVED LONG SHORT-TERM MEMORY PREDICTION MODEL

LSTM is a variation of RNN, which is used to solve the vanishing and exploding gradient problem of the RNN. The LSTM neurons replace the RNN neurons in the hidden layer with LSTM neurons, which can empower the model for long-term memory. It can learn long-term dependencies and works well on a large variety of problems. The LSTM model structure is shown in Fig. 2.

As shown in Fig. 2, the LSTM has a chain-like structure. The input sequence x_t value can affect the output of a long-term distant h_t; the neuron's output date at the last

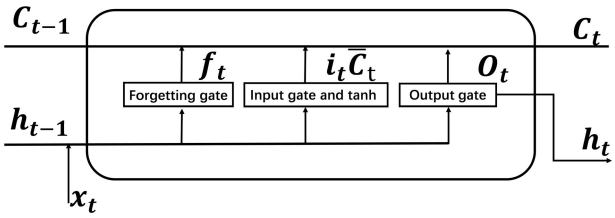

FIGURE 2. Internal structure of the LSTM.

moment and the input at the current moment are entered into the first interaction layer; the forgetting gate layer, and the forgetting gate processes the output f_t, the value is a number from 0 to 1, which is positively correlated with the importance. The interaction layer is the input gate layer, the data at the previous moment, and the current input are processed by the input gate to determine which information should be updated into the memory unit; after the input gate calculation is completed, a candidate value $\tilde{C}_t$ is created to change the current state; the C_t gate's calculated validated into the overall sequence memory unit, and then the memory unit is updated; by combining the forget gate's calculation result and the calculation result of the input gate, the updated value can be obtained. The symbol indicates that the element is multiplied. The output value of the LSTM in the current state is generated from the data at the previous moment and the current input. Based on the memory unit's update, the final output value of the LSTM is determined. The expression of the gate structure is

$$\begin{cases} f_t = \sigma\left[W_f \cdot (h_{t-1}, x_t) + b_f\right] \\ i_t = \sigma\left[W_i \cdot (h_{t-1}, x_t) + b_i\right] \\ \bar{C} = \tanh\left[W_c \cdot (h_{t-1}, x_t) + b_c\right] \\ C_t = f_t \circ C_{t-1} + i_t \circ \tilde{C}_t \\ o_t = \sigma\left[W_o \cdot (h_{t-1}, x_t) + b_0\right] \\ h_t = 0_t \circ \tanh\left(C_t\right) \end{cases}, \quad (1)$$

where f_t, i_t, and o_t are the outputs of three sigmoid functions σ; W_f, W_i, W_c, and W_o are the weights applied to the concatenation of the new input x_t; output h_{t-1} are obtianed from previous cell; b_f, b_i, b_c, and b_o are the corresponding biases.

The cell composition of the neural networks is shown in Fig. 3.

The basic structure of a standard LSTM neural network is shown in Fig. 3(a); The basic structure of the improved LSTM with dropout is shown Fig. 3(b). In the improved LSTM, the neurons in the hidden layer are temporarily deleted randomly according to the set probability during training. The unconnected neurons are temporarily deleted after dropout, and then the training process is standard. The input value is propagated forward, and the loss value is propagated back. After training, the weight and bias of the neurons which have not been deleted are updated, and the deleted neurons are restored. The above processes are repeated until convergence.

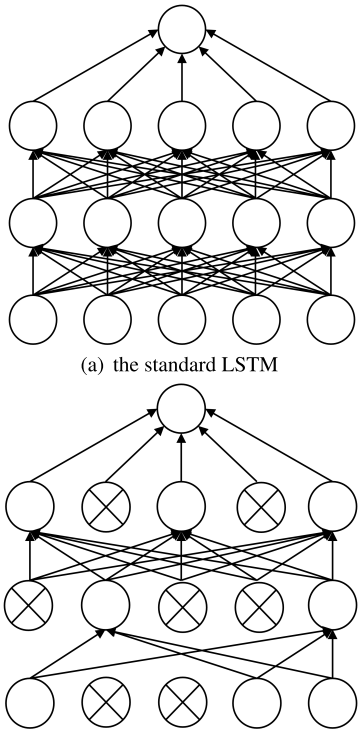

(a) the standard LSTM

(b) the improved LSTM with dropout

FIGURE 3. Randomly deactivated layer of neural network.

The calculation formula of the improved LSTM after adding dropout is

$$\begin{aligned} \tilde{y}^{(l)} &= r^{(l)} \cdot y^{(l)} \\ z_i^{(l+1)} &= w_i^{(l+1)} \tilde{y}^{(l)} + b_i^{(l+1)} \\ y_i^{(l+1)} &= f\left(z_i^{(l+1)}\right), \end{aligned} \tag{2}$$

where w_i denotes the weight of each neuron; $\tilde{y}^{(l)}$ denotes the output of neurons through the inactivated layer; r denotes the random probability generated by Bernoulli function, r denotes a random probability of 0-1; b_i denotes bias; $z_i^{(l+1)}$ denotes the output of the neuron at the next moment; $y_i^{(l+1)}$ denotes the output of neuron after excitation function. In the hidden layer of the improved LSTM, the neuron is randomly inactivated, which can prevent overfitting in the prediction.

After the dropout layer effect, the LSTM hidden layer's output is connected to a fully connected dense layer, and each neuron that has been randomly inactivated is connected to the neuron in the dense layer. This paper can get the predicted value of heave motion after activation by the activation function, thought to multiply the hidden layer's output by a matrix, and add a bias term. Setting the fully connected dense layer is because the predicted value contains the characteristic information of the heave motion initially, a fully connected layer is still needed to realize the learning of the functional relation of vessel between historical data and the predicted result. The full connection can learn the functional relation of vessel between historical data and prediction results, which is shown as follows:

$$h_t^D = W_p h_t^L + b, \tag{3}$$

where W_p denotes the weight between the LSTM layer and the full connection after dropout; h_t^L denotes the output of the LSTM layer at the t^{th} time; h_t^D denotes the output of the LSTM layer at $t + 1^{th}$ time.

C. PARAMETER SETTING

According to the characteristics of the vessel heave sequence, an improved LSTM structure is established. The improved LSTM comprises a five-layer network, including the input layer, the hidden layer (LSTM layer), the dropout layer, the fully connected feedback layer, and the final regression layer. To improve the control accuracy of the vessel, reducing data overfitting, some parameters are set as follows:

1) STEP SIZE SELECTION OF INPUT DATA IN THE LSTM LAYER

The input of the improved LSTM is one more timestep than other neural networks. The added timestep can be regarded as something that happened in the past or future. The network can predict the next step based on the accumulated state information in the memory unit. When the step length is 0.1 s, the research can select 1-20 steps for input each time to obtain the corresponding predicted value. If the datum of the history sequence are too short, they can cause the network to calculate more iterations in the prediction process. If the calculation time is too long, and it can lead to reduced accuracy.

2) SELECTION OF THE NUMBER OF NEURONS IN THE LSTM LAYER

The number of neurons can directly affect the prediction accuracy of the network. A large number of neurons can cause some problems as follows: it can increase the calculation time, cause excellent performance in the training process, and cause overfitting in the prediction process. A small number of elements can make under-fitting occurred. The selection of the number of neurons is generally determined by trials and errors. After abundant experiments in heave motion prediction, the number of hidden nodes for the improved LSTM is decided as 200.

3) SETTING OF OTHER PARAMETERS IN THE IMPROVED LSTM

The adaptive moment estimation solver is selected in this paper. The solver has the advantages of performing a step-wise optimization on a random objective function, having high computational efficiency, and requiring a small memory footprint. The initial learning rate is 0.005, and after half of the training is multiplied by 0.2 to reduce the learning rate to prevent fluctuations at the optimal solution. The gradient threshold is set to 1 to prevent data from growing too fast due to the gradient explosion. The dropout probability of neurons

in the dropout layer is 0.2. Since the gate unit setting in the LSTM network makes the gate's output, a number from 0 to 1, tanh is used as the activation function.

III. DATA RESORCES

This Section introduces the data sources, mainly including the waves modeling and the vessel modeling. The obtained vessels heave motion sequence can be the input vector of the prediction model.

A. WAVE MODEL WITH ITTC SPECTRUM

In the marine operation, when the sea state is greater than 5, the vessel's speed and direction can be greatly affected by the environment, and navigation is dangerous, so it is not recommended to sail out. When the sea state is less than 3, the impact on the vessel is small. As a result, this paper studies the vessel heave motion response from sea state 3 to sea state 5.

1) WAVE MODEL

Waves are low-frequency motion systems with strong randomness. In this respect, waves are regarded as a superposition of several waves from different directions, the structure of motion response is linear. The wave propagation characteristics in all directions are ignored in the simplified model. The wave only propagates in a fixed direction, which is regarded as the linear superposition of infinite harmonics. For long peaked irregular waves, the instantaneous wave height can be expressed as

$$\zeta(t) = H + \sum_{i=1}^{\infty} \zeta_{a_i} \cos\left(k_i \xi - \omega_i t + \varepsilon_i\right), \tag{4}$$

where ζ_{a_i} denotes the regular wave amplitude; k_i denotes the wave number; ω_i denotes the frequency; ε_i denotes the phase angle; H denotes the fixed tide height of the sea surface.

By assuming that the tidal height of the sea surface is constant, $H = 0$, the $\zeta(t)$ can be expressed as

$$\zeta(t) = \sum_{i=1}^{\infty} \zeta_{a_i} \cos\left(\omega_i t + \varepsilon_i\right). \tag{5}$$

2) THE ENERGY EQUALIZATION METHOD

By Eq.(5), it can be seen that the wave model is expressed as the sum of the harmonics. If the frequency, amplitude, and initial phase of the harmonics are determined, the wave model can be established.

The principle of the energy equalization method is shown in Fig. 4. In order to segment the wave frequency with equal energy, the number of frequencies after segmentation can tend to infinity. Δw_i tends to infinity, the wave after segmentation can be regarded as the harmonic with a fixed frequency. The wave model can be obtained by superimposing the harmonics after several times segmentation. The frequency of the segmented wave is $w_1, w_2, w_3, \ldots, w_n$, which can be substituted into the wave energy spectrum S. The spectrum $S(w_1), S(w_2), S(w_3), \ldots, S(w_n)$ are obtained by

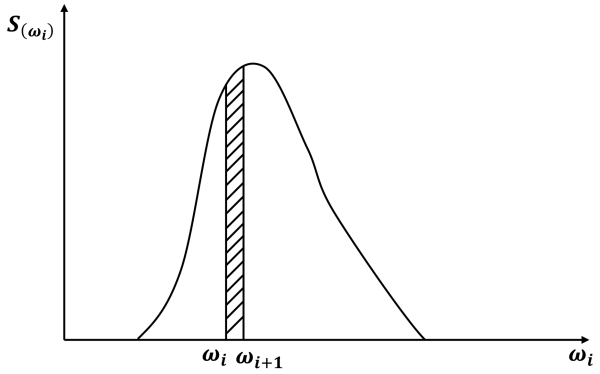

FIGURE 4. The principle of energy equalization method.

$$\int_{\omega_0}^{\omega_1} S(\omega_i)\,\mathrm{d}\omega_i = \int_{\omega_1}^{\omega_2} S(\omega_i)\,\mathrm{d}\omega_i = \cdots = \int_{\omega_{n-1}}^{\omega_n} S(\omega_i)\,\mathrm{d}\omega_i. \tag{6}$$

The wave amplitude ζ_{a_i} can be obtained by the frequency spectrum ω_i. According to the relationship between amplitude and energy, the amplitude of each harmonic can be expressed as:

$$\sum_{\Delta\omega} \frac{1}{2}\zeta_{a_i}^2 = S(\omega_i)\,\Delta\omega_i, \tag{7}$$

where $\Delta\omega_i = \mathrm{d}\omega_i = \omega_i - \omega_{i-1}$. Further,

$$\zeta_{a_i} = \sqrt{2\int_{\omega_{i-1}}^{\omega_i} S(\omega_i)\,\mathrm{d}\omega_i}. \tag{8}$$

According to the International Towing Tank Conference (ITTC) parameter spectrum, the $S(\omega_i)$ is

$$S(\omega_i) = \frac{A}{4MB\Delta\omega_i}. \tag{9}$$

3) ITTC TWO-PARAMETER WAVE SPECTRUM

The energy equalization method is used to establish the waves model. Therefore, the vessel heave motion response to this model is calculated. The wave spectrum uses the ITTC single-parameter spectrum. The relation between the instantaneous value and time of the fixed-point long-peak wave simulation of the ITTC single-parameter spectrum is in Eq. (10):

$$\zeta(t) = \sqrt{\frac{A}{2BM}} \sum_{i=1}^{M} \cos\left(\omega_i t + \varepsilon_i\right), \tag{10}$$

where $\mathrm{A} = 0.78, \mathrm{B} = \frac{3.12}{h_e}$; h_e denotes the significant wave height; the selected frequency division number denotes uniformly distributed; M denotes number of segments for the selected frequency; ε_i denotes the random phase of the i^{th} time harmonics, which is evenly distributed between 0 and 2π.

In the energy spectrum, h_e and ω_i are important parameters. In order to research the effect factors of the wave model,

TABLE 1. Classifications of wave level.

Sea state	Significant wave height (m)
1	< 0.1
2	0.1 - 0.5
3	0.5 - 1.25
4	1.25 - 2.5
5	2.5 - 4.0
6	4.0 - 6.0
7	6.0 - 9.0
8	9.0 - 14.0
9	> 14.0

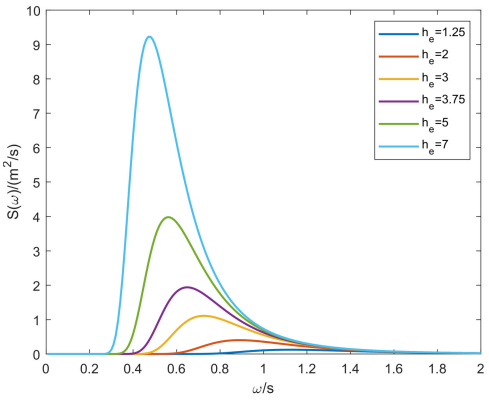

FIGURE 5. Wave energy spectrum at different significant wave heights.

the wave energy spectrums at different significant wave heights and different angular frequencies are researched.

According to the regulations of the State Oceanic Administration, the sea conditions are divided into nine levels, which are shown in Table 1.

Fig. 5 shows wave energy spectrums. The significant wave height $h_e = 1.25$ m, $h_e = 2$ m, $h_e = 3$ m, $h_e = 3.75$ m, $h_e = 5$ m, and $h_e = 7$ m are discussed. The ω_i is set from 0 to 2 rad/s. It can be seen that the spectral density with different h_e is different. When the h_e increases, the overall energy of the wave also increases. The results show that the greater significant wave height, the greater maximum value of the spectral density. At the end, the spectral density first increases and then decreases after a certain frequency during the same h_e.

The principle of energy equalization method is the superposition of different regular waves. The simulation accuracy can increase with the increase of regular wave number M. However, M cannot be taken as infinity. The larger the M, the slower the calculation speed. When M is 30, it can meet the needs of the accuracy and meet the prediction accuracy in vessel motion. $M = 10$ and $M = 50$ for signal simulation and verification are discussed in this paper.

Fig. 6 shows the comparison between the wave energy spectrum and the theoretical wave energy spectrum. It can be seen that the four simulated wave models basically conform to the statistical principles of real wave conditions. The wave model has all states of ergonomics; when the simulation time is long enough, all the model characteristics of the wave can be described. For the sea area on the same sea state,

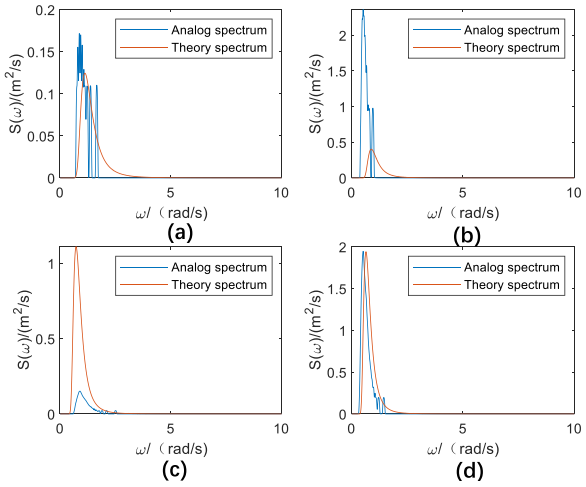

FIGURE 6. Comparison of analog spectrum and theoretical spectrum, (a) the superimposition of 10 regular waves at sea state 3, (b) the superimposition of 10 regular waves at sea state 5, (c) the superimposition of 50 regular waves at sea state 3, (d) the superimposition of 50 regular waves at sea state 5.

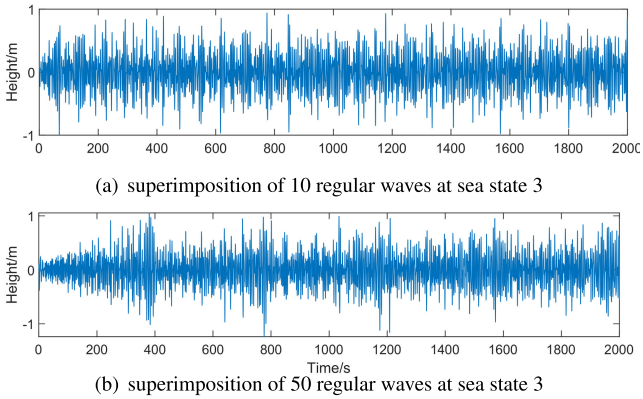

FIGURE 7. Wave model at sea state 3.

the data of 20 minutes of general fixed-point measurement can basically reflect the wave conditions in the area. After the fixed-point wave is decomposed, each unit's regular wave amplitude is basically the same, and the initial phase of each wave falls on.

In detail, the wave model is shown in Fig. 7 at sea state 3 with $h_e = 1.25$ m, the wave model is shown in Fig. 8 at sea state 5 with $h_e = 3.75$ m. Compared Figs. 7 with 8, it can been seen that as the significant wave height h_e increases, the average wave height value increases, and the waves become more intense. This paper can see the height is from -1 m to 1 m at sea state 3 and the height is from -4 m to 4 m at sea state 5.

As a result, the effective wave height can be used to reflect the intensity of the waves and simulate the sea conditions, which is of great significance to vessels motion control.

The wave model based on the energy equal equalization method shows that the wave model is linearly superimposed by different unit regular waves. The results reflect the statistical characteristics of waves. The ocean surface can move

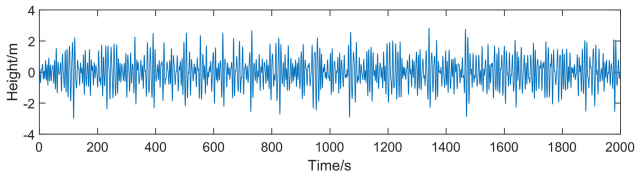

(a) superimposition of 10 regular waves at sea state 5

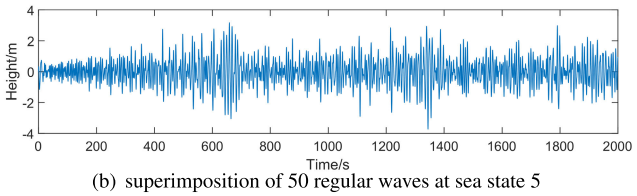

(b) superimposition of 50 regular waves at sea state 5

FIGURE 8. Wave model at sea state 5.

TABLE 2. Evaluation index of wave motion.

Energy equalization	MV ($\times 10^{-16}$)	S	K
10 waves at sea state 3	-3.56730	-0.055	2.8622
10 waves at sea state 5	-0.83795	-0.0107	2.9882
50 waves at sea state 3	-67.17600	-0.0156	3.4631
50 waves at sea state 5	25.04200	0.0186	4.0672

TABLE 3. Principal particulars and hydrodynamic parameters of "Yuming".

Descriptions	Parameter	Unit	Value
Vessel length	L	m	189.9
Vessel width	B	m	32.26
Vessel depth	D	m	15.7
Vessel draft	d	m	10.3
Full-load drainage volume	V	T	48000
Vessel speed	u	m/s	0
Heading	α	°	0
Waterline area	Cs	m²	6126.174
Additional mass of heave motion	Izz	kg	4897959.2
Heave natural circular frequency	w	rad/s	6.28
Dimensionless attenuation coefficient	/	/	7.045

and change with time. This paper defines sea level as the base level, mean value (MV) of the ocean surface is zero, and it is symmetrical. According to statistical principles, the standard distribution skewness is 0, and the kurtosis (K) is 3. The mean value of wave surface motion, skewness (S), and kurtosis of the waves simulated by the energy equal division method are shown in Table 2.

It can be seen from Table 2 that when the number of regular waves is in the unit, the simulated wave energy spectrum has obvious burrs. When the number of regular waves increases, the burr phenomenon has a significant improvement, but the overall trends of vessel motion and wave model are the same. There can be no particularly low or high-frequency bands, most of them are concentrated in the same frequency band. As the significant wave height increases, its frequency also decreases. By taking the vessel named "Yuming" of Shanghai Maritime University as a reference, the specific parameters are shown in Table 3:

B. VESSEL MOTION MODEL

Due to the complex sea environment, vessels are affected by irregular waves. In the actual vessels motion, the 6-DOF

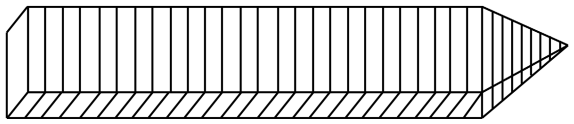

FIGURE 9. Vessel motion model based on strip theory.

motion on the vessels are coupled with each other. The lateral and longitudinal motion are couplings, but the calculation is very complicated. By considering the complex coupling motion of vessels at sea when it is combined with the actual vessels, it is necessary to simplify the model to eliminate the interference of weak factors. The following assumptions are employed:

1) The complex wave model is simplified and replaced by the dual-parameter spectrum.
2) The waves are of small amplitude, the vessel motion caused by waves is also a slight motion.
3) A vessel is rigid a slender and rigid body, ignoring its elastic effects.
4) For having high real-time performance, the vessel heave motion is simplified as an independent motion, ignoring the coupling of each vessel motion.

The vessel motion model based on strip theory is seen in Fig. 9. In strip theory, the hull is divided into several small thickness cross sections. When each cross section is calculated, the cross section is only subjected to a two-dimensional fluid force, so the three-dimensional flow of fluid to the vessel becomes a two-dimensional flow on each slice cross section. The forces on each slice cross section can be calculated. Finally, all cross sections are integrated with the length of the vessel, the three-dimensional force of fluid to the vessel is calculated.

The coupled vessel motion model in the longitudinal and pitching is

$$\begin{cases} (m + a_{33})\,\ddot{z} + b_{33}\dot{z} + c_{33}z + a_{35}\ddot{\theta} + b_{35}\dot{\theta} + c_{35}\theta = Z_3 \\ (I + a_{55})\,\ddot{\theta} + b_{55}\dot{\theta} + c_{55}\theta + a_{53}\ddot{z} + b_{35}\dot{z} + c_{35}z = M_5, \end{cases} \tag{11}$$

where z and θ represent the heave displacement and pitch angle of the vessel in longitudinal motion, respectively; $\dot{z}$ and $\dot{\theta}$ are the heave velocity and pitch angular velocity; $\ddot{z}$ and $\ddot{\theta}$ are the heave acceleration and pitch angular acceleration; I is the pitch moment of inertia; a_{ij}, b_{ij}, c_{ij} $(i, j = 3, 5)$ are the hydrodynamic coefficient, depending on the parameters of the vessel.

The motion of vessels are similar to energy converter in waves. The wave energy is used as the input signal, which is converted by the vessel and output multi degree of freedom motion of vessels. Conversion of wave energy to vessel motion is shown in Fig.10.

Relationship between wave height and vessel motion is in Eq. (11). The heave motion can be simplifying:

$$\ddot{z} + 2\nu_{zz}\dot{z} + n_{zz}^2 = \frac{F_{zz}}{D/g + \lambda_{zz}}, \tag{12}$$

FIGURE 10. Conversion of wave energy to vessel motion.

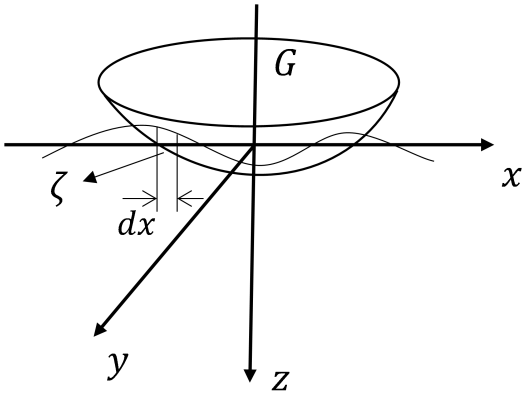

FIGURE 11. The disturbing force on vessel heave motion.

where $2v_{zz}$ is damping coefficient of heave motion.

$$2v_{zz} = \frac{2N_{zz}}{\frac{D}{g} + \lambda_{zz}}, \tag{13}$$

where $2N_{zz}$ denotes the damping force (or moment) coefficient, and $2N_{zz} = fS_w$; f denotes the dimensionless coefficient, $f = 0.18$; S_w denotes the waterline area of the vessel; D denotes the mass of vessel; g denotes the acceleration of gravity; F_{zz} denotes the heave disturbing force of wave to vessel; λ_{zz} denotes the additional mass of the heave motion; natural circular frequency of heave n_{zz} is

$$n_{zz} = \sqrt{\frac{\rho g S_w}{\frac{D}{g} + \lambda_{zz}}}, \tag{14}$$

where ρ is the density of seawater.

The disturbing force on vessel heave motion generated by waves is shown in Fig.11.

Fig. 12 shows the vessel board coordinate system used in this paper. In coordinate system $o - xyz$, the center of gravity of the vessel o is the origin of the coordinate system; the x-axis points the vessel surge direction; the y-axis points the vessel sway direction; h, u, and v denote heave velocity, surge velocity, sway velocity, respectively; the direction of h, u, and v are along the z-axis, along the x-axis and along the y-axis in the system, respectively; φ (roll rate), θ (pitch rate), ψ (yaw rate), which are around x-axis, y-axis and around z-axis in the system, respectively.

The vessel heave motion established by strip theory in waves is

$$z(t) = \sum_{i=1}^{n} z_{0i}\zeta_a, \tag{15}$$

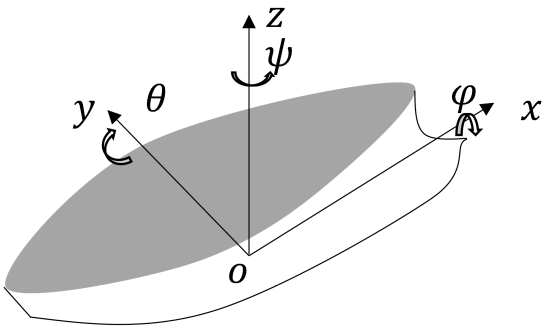

FIGURE 12. Vessel motion model.

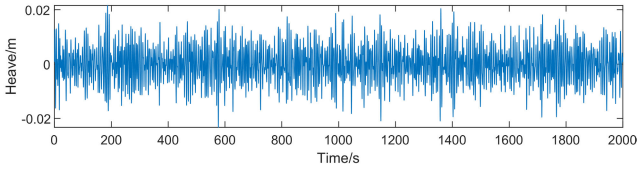

FIGURE 13. Superimposition of 50 regular waves and the corresponding vessel heave motion at sea state 3.

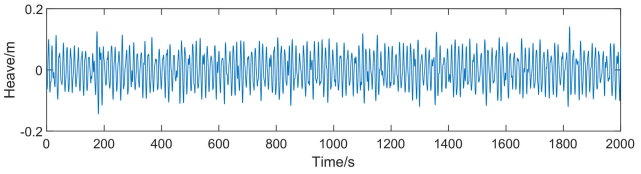

FIGURE 14. Superimposition of 50 regular waves and the corresponding vessel heave motion at sea state 5.

By combining with Eq. (10), the heave motion in Eq. (15) can be expressed as:

$$z(t) = \sum_{i=1}^{n} z_{0i}\sqrt{\frac{A}{2BM}}\cos\left(\omega_i t + \varepsilon_i\right), \tag{16}$$

where $z_{0i} = \zeta_a|W_z(i\omega)|$; $|W_z(i\omega)|$ is the amplitude-frequency response function of the heave motion.

After the vessel motion equation under the regular wave of the unit is obtained, the decomposed wave can be superimposed on the vessel heave motion according to the linear superposition principle. The speed is 0 m/s and the angle of encounter is 0°, vessel motion response to waves can be obtained. After solving Eq. (16), the curve of veseel vessel heave motion are is shown in Figs. 13 and 14. By comparing Fig. 13 with Fig. 7 (b), and Fig. 14 with Fig. 8 (b), it can been seen that the vessel can eliminate part of the influence from the wave. The results show that changing trend of the vessels heave motion have a certain positive correlation with the waves motion.

As a result, the significant wave height is an important factor affecting the vessel heave motion.

C. MODEL EVALUATION INDEX

The neural network's performance in the prediction can be seen by comparing the predicted value with the real value, its accuracy can be seen intuitively and clearly by quantifying it.

When compared with the accuracy of other prediction algorithms, the evaluation index can objectively get the degree of agreement between different algorithms and actual data. Three indexes are used to measure the performances of the different methods for vessel heave motion prediction, including the root mean square error (RMSE), the mean absolute error (MAE), and the mean absolute percentage error (MAPE), which are defined as follows:

1) ROOT MEAN SQUARE ERROR (RMSE)

RMSE is the root of the mean square error, which is more intuitive than the mean square error in the order of magnitude. The RMSE is

$$E_{\mathrm{RMSE}} = \sqrt{\frac{1}{\mathrm{n}}\sum_{i=1}^{\mathrm{n}}\left(y_{pi} - y_{ti}\right)^2}, \tag{17}$$

where y_{pi} is the predicted value at i^{th} time, i = 1,2...n; y_{ti} is the real value at i^{th} time, and n is the number of time steps.

2) MEAN ABSOLUTE ERROR (MAE)

MAE describes the average of the absolute values of the difference between the model's predicted value and the observed value. MAE can be expressed by

$$E_{\mathrm{MAE}} = \frac{1}{\mathrm{n}}\sum_{i=1}^{\mathrm{n}}\left|y_{pi} - y_{ti}\right|. \tag{18}$$

3) MEAN ABSOLUTE PERCENTAGE ERROR (MAPE)

MAPE describes the percentage of error between the predicted value and the true value. Compared with the MAE, the degree of deviation between the model and the true value can be seen more intuitively. MAPE can be expressed by

$$E_{\mathrm{MAPE}} = \frac{1}{\mathrm{n}}\sum_{i=1}^{\mathrm{n}}\left|\frac{y_{pi} - y_{ti}}{y_{ti}}\right| \times 100\%, \tag{19}$$

IV. RESULTS AND DISCUSSION

In order to study the influence of sea states on vessel heave motion prediction and verify the correctness of the model, this paper takes the ''Yuming'' of Shanghai Maritime University as an example. Time delay is an important parameter, this paper studies the effect of vessel prediction from sea state 3 to sea state 5 with different predicted time series. Predicted time series is the time span used to predict time series in the future. In this paper, the predicted time series is n seconds, meaning that predicting applied vessel heave motion in n seconds ahead by the improved LSTM. The value of the predicted time series is equal to the delay time of the system.

In the control system of wave compensation equipment, the time delay of different devices is different because of the controller and actuator. The causes of system delay mainly include mechanical system delay and drive system delay. By taking the series-parallel hybrid platform of Shanghai Maritime University as an example, the problem of time delay studied in this paper is to improve the system control of the hybrid platform. In respect of mechanical system delay, the hybrid mechanism belongs to the medical platform, a special kind of compensation equipment, which improves the safety of marine medical facilities. Compared with the large wave compensation platform, the load and inertia of the platform are small, so the mechanical system delay is small. In respect of drive system delay, compared with hydraulic drive and mechanical drive, the precision of electrical drive is high, so the time delay is relatively less. Besides, the time delay is only a set parameter, which can be adjusted for different time-delay systems. Considering the above aspects, the time delay of the compensation platform is about 0.27 s, so the prediction predicted time series is 0.1 s, 1 s, and 2 s respectively for comparison.

A. MODEL TRAINING

90% of the heave datum are trained by the network, and the remaining 10% are used to verify the prediction accuracy of the network. The rolling prediction is used in the data prediction. The network outputs the prediction after the data of the training set. Every time the next step heave displacement is predicted. The real displacement value of the previous step is taken as the input. To predict the data at t^th time, the training steps of the model are as follows:

Step 1: Input the data of t = n (n is the beginning time of training) into the input layer of LSTM, and output the activated result through tanh.

Step 2: The processed results are input into the LSTM hidden layer, and the data is processed continuously through the gate unit, and the processed data is output to the random deactivation layer.

Step 3: The data is randomly inactivated, and the neurons are randomly deleted and restored continuously, and the weights are updated to converge.

Step 4: The data passing through the random deactivation layer is input into the full connection layer to realize the function learning between the historical data and the prediction results.

Step 5: Input data to the output layer for output.

Step 6: The residual between the output value and the real value of the training set is calculated.

Step 7: Update the weight by back-propagation through time (BPTT).

Step 8: The data of t = n and the state of t = n + 1 memory unit are input into the input layer of LSTM, and the activated result is output through tanh.

Step 9: Repeat the above process until t = t − 1.

Step 10: The predicted value at time t is output.

B. SEA STATE 3 PREDICTION

In the model prediction, three models are used to predict the vessel heave and motion, which are the traditional fully connected BP, the standard LSTM, and the improved LSTM with dropout. The BP network is a three-layer network, and the number of neurons is 7 after trial and error. In detail,

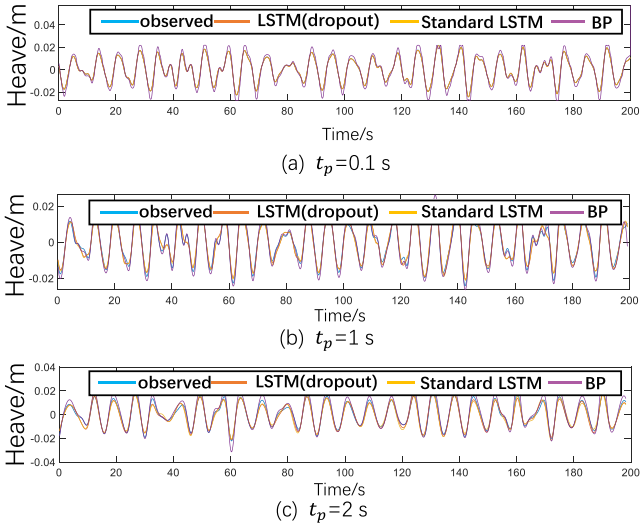

FIGURE 15. Comparison of prediction with algorithm results at sea state 3.

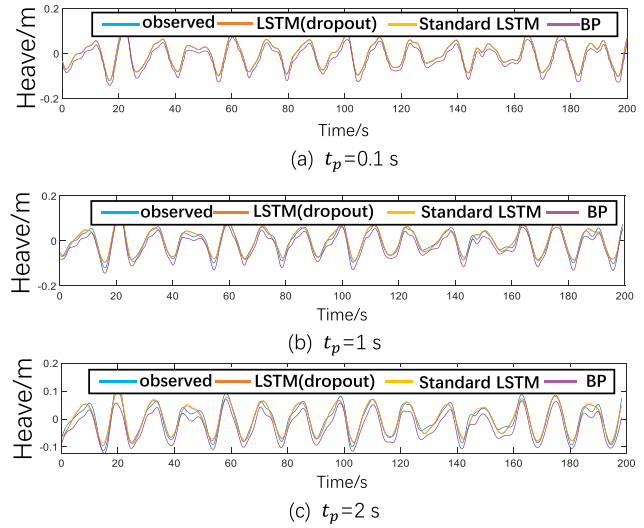

FIGURE 16. Comparison of prediction with algorithm results at sea state 5.

the prediction predicted time series (t_p) are 0.1 s, 1 s, and 2 s, respectively. The prediction result of the model at sea state 3 is shown in Fig. 15.

C. SEA STATE 5 PREDICTION

In order to further study the influence of significant wave height on the prediction of vessel motion, this paper compared it with sea state 5. The prediction results of vessel heave motion direction after 10 regular wave superposition and 50 regular waves superposition are discussed, respectively.

D. RESULTS AND DISCUSS

Figs. 15 and 16 show the prediction comparisons of the three neural networks algorithm, respectively. It can be seen from the figures that three neural networks perform well in the 0.1 s prediction process of the sea state 3 predictions. In the case of sea state 5, and after lengthening the prediction time,

TABLE 4. Prediction errors of vessel heave motion at t_p = 2 s.

Sea states	sea state 3			sea state 5		
Algorithm	MAE	RMSE	MAPE	MAE	RMSE	MAPE
BP	0.0022	0.0026	0.1426%	0.0282	0.0290	0.085%
Standard LSTM	0.0015	0.0019	0.0487%	0.0078	0.0093	0.0478%
Improved LSTM	0.0014	0.0019	0.0443%	0.0076	0.0089	0.0368%

TABLE 5. Prediction errors of vessel heave motion at t_p = 1 s.

Sea states	sea state 3			sea state 5		
Algorithm	MAE	RMSE	MAPE	MAE	RMSE	MAPE
BP	0.0022	0.0026	0.1023%	0.0180	0.0194	0.0469%
Standard LSTM	0.0013	0.0016	0.0163%	0.0047	0.0057	0.0122%
Improved LSTM	0.0012	0.0015	0.0142%	0.0045	0.0055	0.0079%

TABLE 6. Prediction errors of vessel heave motion at t_p = 0.1 s.

Sea states	sea state 3			sea state 5		
Algorithm	MAE	RMSE	MAPE	MAE	RMSE	MAPE
BP	0.0022	0.0026	$1.06 \times 10^{-2}\%$	0.0200	0.0260	$1.7 \times 10^{-3}\%$
Standard LSTM	0.0019	0.0008	$1.43 \times 10^{-4}\%$	0.0005	0.0007	$7.51 \times 10^{-6}\%$
Improved LSTM	0.0006	0.0001	$7.7 \times 10^{-5}\%$	0.0003	0.00004	$6.34 \times 10^{-5}\%$

the improved LSTM is significantly improved than the BP neural network. This is because the gate unit in the improved LSTM retains the previous state information, while the neurons in the BP neural network are independent of each other.

To intuitively quantify the prediction accuracy of the neural network, the prediction and evaluation index tables of the neural network for the vessel heave motion at various sea states are shown in Tables 4, 5, and 6.

From the analysis of Tables 4, 5, and 6, it can be seen that the prediction accuracy of the improved LSTM is better than the traditional BP network and the standard LSTM. A certain improvement. In the prediction of vessel heave motion response of 2 s, 1 s, and 0.1 s, MSE of the LSTM with dropout layer at sea state 3 reached 1.4×10^{-3}, 1.2×10^{-3}, and 6.44×10^{-5}; RMSE reached 1.9×10^{-3}, 1.5×10^{-3}, and 6.44×10^{-5}, and MAPE reached $4.43 \times 10^{-2}\%$, $1.42 \times 10^{-2}\%$, $7.51 \times 10^{-6}\%$, and the root mean square at sea state 5. MSE reached 7.6×10^{-3}, 4.5×10^{-3}, and 3.72×10^{-4}, RMSE reached 8.9×10^{-3}, 5.5×10^{-3} and 4.71×10^{-4}. MAPE reached $3.68 \times 10^{-2}\%$, $7.9 \times 10^{-3}\%$ and $6.34 \times 10^{-5}\%$. By comparing with the BP network and standard LSTM network, it can be found that the accuracy has been improved to a certain extent, and it can be seen that the smaller the time step of each prediction, the higher the prediction accuracy. When the prediction time increases, the error appears to increase. The improved LSTM with dropout has the ability to prevent overfitting. As a result, the prediction of vessel heave motion based on the improved LSTM performs well, which provides a new idea for solving the time delay problem in wave compensation.

V. CONCLUSION

The prediction of vessel heave motion is key to solve the problem of time delay in the wave compensation control system. A short vessel heave motion prediction based on the improved LSTM has been studied in this paper.

Firstly, the algorithm flow is introduced. Then the wave and vessel are modeled. Finally, the vessel heave motion is predicted under different time delay conditions and different sea conditions. By comparing and analyzing the prediction results of the different neural network models, the following conclusions can be drawn:

1) The improved LSTM can accurately predict the heave motion based on time history datum. Besides, the RMSE between the predicted and actual values is less than 0.003, and no over-fitting occurred.
2) The improved LSTM has a certain effect in short-term prediction to solve the problem of time delay in wave compensation.
3) The smaller the predicted time series, the higher the prediction accuracy in short-term prediction can be obtained.

Consequently, the time series prediction algorithm based on the improved LSTM model has better application value in the actual environment that is considered in this study. The improved LSTM network is more targeted and has better adaptability in the field of vessel heave motion prediction.

REFERENCES

[1] J. K. Woodacre, R. J. Bauer, and R. A. Irani, "A review of vertical motion heave compensation systems," *Ocean Eng.*, vol. 104, pp. 140–154, Aug. 2015.

[2] X. Hu, F. Li, and G. Tang, "Kinematics analysis of 3UPU_UP coupling parallel platform in the marine environment," *IEEE Access*, vol. 8, pp. 158142–158151, 2020.

[3] V. Piscopo, A. Scamardella, and S. Gaglione, "A new wave spectrum resembling procedure based on ship motion analysis," *Ocean Eng.*, vol. 201, Apr. 2020, Art. no. 107137.

[4] M. W. Li, J. Geng, D. F. Han, and T. J. Zheng, "Ship motion prediction using dynamic seasonal RvSVR with phase space reconstruction and the chaos adaptive efficient FOA," *Neurocomputing*, vol. 174, pp. 661–680, Jan. 2016.

[5] Y. Dai, R. Cheng, X. Yao, and L. Liu, "Hydrodynamic coefficients identification of pitch and heave using multi-objective evolutionary algorithm," *Ocean Eng.*, vol. 171, pp. 33–48, Jan. 2019.

[6] L. M. Huang, W. Y. Duan, Y. Han, D. H. Yu, and A. Elhandad, "Extending the scope of AR model in forecasting non-stationary ship motion by using AR-EMD technique," *J. Ship Mech.*, vol. 19, no. 9, pp. 1033–1049, 2015.

[7] S. Duan, Q. Ma, L. Huang, and X. Ma, "A LSTM deep learning model for deterministic ship motions estimation using wave-excitation inputs," in *Proc. 29th Int. Ocean Polar Eng. Conf.*, 2012, pp. 959–965.

[8] J. Wessberg, C. R. Stambaugh, J. D. Kralik, P. D. Beck, M. Laubach, J. K. Chapin, J. Kim, S. J. Biggs, M. A. Srinivasan, and M. A. L. Nicolelis, "Real-time prediction of hand trajectory by ensembles of cortical neurons in primates," *Nature*, vol. 408, no. 6810, pp. 361–365, Nov. 2000.

[9] X. Fei, C.-C. Lu, and K. Liu, "A Bayesian dynamic linear model approach for real-time short-term freeway travel time prediction," *Transp. Res. C, Emerg. Technol.*, vol. 19, no. 6, pp. 1306–1318, Dec. 2011.

[10] Y. Liu, W. Duan, L. Huang, S. Duan, and X. Ma, "The input vector space optimization for LSTM deep learning model in real-time prediction of ship motions," *Ocean Eng.*, vol. 213, Oct. 2020, Art. no. 107681.

[11] Z. Nie, F. Shen, D. Xu, and Q. Li, "An EMD-SVR model for short-term prediction of ship motion using mirror symmetry and SVR algorithms to eliminate EMD boundary effect," *Ocean Eng.*, vol. 217, Dec. 2020, Art. no. 107927.

[12] J.-C. Yin, A. N. Perakis, and N. Wang, "A real-time ship roll motion prediction using wavelet transform and variable RBF network," *Ocean Eng.*, vol. 160, pp. 10–19, Jul. 2018.

[13] P. Naaijen, R. R. T. Van Dijk, R. H. M. Huijsmans, and A. A. El-Mouhandiz, "Real time estimation of ship motions in short crested seas," in *Proc. Int. Conf. Offshore Mech. Arctic Eng.*, vol. 43444, 2009, pp. 243–255.

[14] Y. Su, J. Lin, D. Zhao, C. Guo, C. Wang, and H. Guo, "Real-time prediction of large-scale ship model vertical acceleration based on recurrent neural network," *J. Mar. Sci. Eng.*, vol. 8, no. 10, p. 777, Oct. 2020.

[15] H. Jiang, S. Duan, L. Huang, Y. Han, H. Yang, and Q. Ma, "Scale effects in AR model real-time ship motion prediction," *Ocean Eng.*, vol. 203, May 2020, Art. no. 107202.

[16] U. D. Nielsen, A. H. Brodtkorb, and J. J. Jensen, "Response predictions using the observed autocorrelation function," *Mar. Struct.*, vol. 58, pp. 31–52, Mar. 2018.

[17] M. R. Haddara and J. Xu, "On the identification of ship coupled heave–pitch motions using neural networks," *Ocean Eng.*, vol. 26, no. 5, pp. 381–400, 1998.

[18] L. Li, Z. Gao, and Z.-M. Yuan, "On the sensitivity and uncertainty of wave energy conversion with an artificial neural-network-based controller," *Ocean Eng.*, vol. 183, pp. 282–293, Jul. 2019.

[19] J.-C. Yin, Z.-J. Zou, and F. Xu, "On-line prediction of ship roll motion during maneuvering using sequential learning RBF neuralnetworks," *Ocean Eng.*, vol. 61, pp. 139–147, Mar. 2013.

[20] G. De Masi, F. Gaggiotti, R. Bruschi, and M. Venturi, "Ship motion prediction by radial basis neural networks," in *Proc. IEEE Workshop Hybrid Intell. Models Appl.*, Apr. 2011, pp. 28–32.

[21] G.-F. Fan, L.-L. Peng, W.-C. Hong, and F. Sun, "Electric load forecasting by the SVR model with differential empirical mode decomposition and auto regression," *Neurocomputing*, vol. 173, pp. 958–970, Jan. 2016.

[22] G. D. Masi, R. Bruschi, and F. Gaggiotti, "Short term vessel motion forecasting based on wavelet neural network for wave feed-forward dynamic positioning," in *Proc. 22nd Int. Offshore Polar Eng. Conf.*, 2012, pp. 915–919.

[23] S. Hochreiter and J. Schmidhuber, "Long short-term memory," *Neural Comput.*, vol. 9, no. 8, pp. 1735–1780, 1997.

[24] Z. Chao, F. Pu, Y. Yin, B. Han, and X. Chen, "Research on real-time local rainfall prediction based on MEMS sensors," *J. Sensors*, vol. 2018, pp. 1–9, Jun. 2018.

[25] G. E. Hinton, S. Osindero, and Y.-W. Teh, "A fast learning algorithm for deep belief nets," *Neural Comput.*, vol. 18, no. 7, pp. 1527–1554, Jul. 2006.

[26] Z. Huang, W. Xu, and K. Yu, "Bidirectional LSTM-CRF models for sequence tagging," 2015, *arXiv:1508.01991*. [Online]. Available: http://arxiv.org/abs/1508.01991

[27] K. Greff, R. K. Srivastava, J. Koutnik, B. R. Steunebrink, and J. Schmidhuber, "LSTM: A search space odyssey," *IEEE Trans. Neural Netw. Learn. Syst.*, vol. 28, no. 10, pp. 2222–2232, Oct. 2017.

[28] Y. Wang, "A new concept using LSTM neural networks for dynamic system identification," in *Proc. Amer. Control Conf. (ACC)*, May 2017, pp. 5324–5329.

[29] Y. Yao, L. Han, and J. Wang, "LSTM-PSO: Long short-term memory ship motion prediction based on particle swarm optimization," in *Proc. IEEE CSAA Guid., Navigat. Control Conf. (CGNCC)*, Aug. 2018, pp. 1–5.

[30] S. Fan, N. Xiao, and S. Dong, "A novel model to predict significant wave height based on long short-term memory network," *Ocean Eng.*, vol. 205, Jun. 2020, Art. no. 107298.

[31] J. M. Kennedy, J. J. Ford, F. Valentinis, and T. Perez, "Bayesian inference and prediction of wave-induced ship motion based on discrete-frequency model approximations," *IFAC-PapersOnLine*, vol. 51, no. 29, pp. 104–109, 2018.

[32] S. Chakrabarti, "Empirical calculation of roll damping for ships and barges," *Ocean Eng.*, vol. 28, no. 7, pp. 915–932, Jul. 2001.

[33] M. Amini-Afshar and H. B. Bingham, "Added resistance using Salvesen–Tuck–Faltinsen strip theory and the Kochin function," *Appl. Ocean Res.*, vol. 106, Jan. 2021, Art. no. 102481.

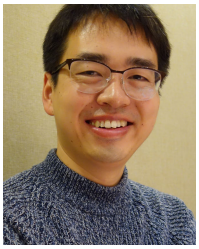

GANG TANG received the master's degree in mechanical engineering from the Harbin Institute of Technology and the Ph.D. degree in mechanical engineering from Shanghai Jiao Tong University. His research interests include artificial intelligence and ocean engineering.

JINMAN LEI received the B.S. degree in mechatronic engineering from Anhui Jianzhu University, Hefei, Anhui, in 2019. She is currently pursuing the M.S. degree in mechanical engineering with Shanghai Maritime University, Shanghai, China. Her research interests include the development of vessel motion control and wave compensation systems.

CHENTONG SHAO is currently pursuing the master's degree in mechanical engineering with Shanghai Maritime University, Shanghai, China. He has published a Chinese science citation database (CSCD) journal article and applies an invention patent. His research interest includes the application of neural network in signal processing.

XIONG HU received the bachelor's and Ph.D. degrees from Shanghai Jiao Tong University. He was a Visiting Professor with the Queensland University of Technology, Australia. He is currently a Professor and a Ph.D. Supervisor with Shanghai Maritime University (SMU), the Dean of the Logistics Engineering College, SMU, and the Dean of the Sino-Dutch Mechatronics Engineering College, SMU. He was responsible for or participated in almost 100 research projects which were sponsored by National Funding Programs, government and both here and abroad enterprises, such as NNSF, 863 program, Dubai Aluminium Company Ltd., Port of Damman, Port of Shanghai, Shanghai Bao Steel Company, ZPMC, and BV. His current research interests include research and teaching works are included in (health) condition monitoring, (remote) control, (condition) assessment, and (maintenance) management of large equipment and its structure, and intelligent processing and prediction of health condition data and signals of machines. In recent years, his major research works are emphasized on the technique development and its application of health condition management, fault diagnosis, safety assessment, and integrated online system of the large hoisting appliances, such as cranes and logistics equipment. He serves as the Executive Director of the Shanghai Mechanical Engineering Society, the Chairman of the Committee of Equipment Condition Monitoring, Assessment and Strategic Decision of the Shanghai Mechanical Engineering Society, the Deputy Director of Branch of Health Condition Monitoring of Shanghai Equipment Management Association, and so on.

WEIDONG CAO received the Ph.D. degree from the College of Environmental Science and Engineering, Hohai University, Nanjing, China, in 2007. He is currently a Professor with the National Research Center of Pumps, Jiangsu University, Zhenjiang, China. His current research interests include fluid dynamics and optimization of fluid machinery.

SHAOYANG MEN received the M.S. degree in communication and information system from the South China University of Technology, in 2014, and the Ph.D. degree in signal and information processing from the University of Nantes, in 2016. His research interests include medical image processing, signal processing, and text information extraction.